

MEASUREMENT OF WINDS AND WAVES FROM A NOMAD BUOY IN HIGH SEASTATES

S.G.P. Skey¹, K. Berger-North¹ and V.R. Swail²

¹Axys Environmental Consulting Ltd.

²Environment Canada, Downsview, Ontario

1.0 INTRODUCTION

In late October 1991 an intense extratropical storm developed in the Atlantic Ocean off the North American coast, and merged with the remnants of Hurricane "Grace". The combined storm, now known as the "Halloween Storm", raged for several days on the Atlantic coastal and offshore regions from Florida to New England and the Maritimes. High seas (waves and surge) affected most of the American and Canadian Atlantic coasts with extensive damage reported along the coast and the loss or damage of several vessels (Bigio, 1992). The high waves generated by the Halloween Storm exceed the 100-year return period at several locations (Cardone and Callahan, 1992).

As a result of this storm, concern was raised as to the ability to predict such extreme wave heights. There has been much speculation on the part of wave modellers that the wind measurements reported by weather buoys may be lower than the actual wind speed existing during high sea conditions. Several possible causes of the lower wind speed measured by the buoys have been advanced, including: sheltering of the buoy's anemometers by the waves; extreme buoy motion; and the methods of data presentation (averaging period and time). However, there is no consensus as to which factor may be the most prominent during high wave conditions, nor the relative magnitudes of these factors.

As a result of the 1991 Halloween Storm, Environment Canada commissioned a hindcasting study. The wind fields used in the hindcast study were generated from observations and pressure gradient fields by Oceanweather Inc. (Cardone and Callahan, 1992; Cardone, 1993, pers. comm.). The observed winds were increased by 5% to adjust the vector-averaged wind speed to a scalar-averaged wind speed following the findings of Gilhousen (1987), and then scaled to 20 m height (Cardone and Callahan, 1992).

The wave hindcasts undertaken by Oceanweather Inc. performed well in predicting peak waves measured at most buoys but could not reproduce the 17.4 m observed maximum significant wave at buoy #44137. Cardone (1993, pers. comm.) felt that a wind speed of 36-39 m/s would be required to generate a 17 m significant wave. The mean wind speed measured concurrent with this wave was 24.7 m/s, while the measured peak wind speed was 35 m/s. Cardone felt that more knowledge is needed of the wind field structure during storms, especially when the pressure gradients are tight. He also noted that several forecasting groups including Environment Canada's Pacific Weather Centre use the peak wind speed rather than the mean in their analyses.

The ability to forecast wave heights accurately during storm conditions is a prime objective for increasing marine and coastal safety. Accurate determination of wave properties during extreme weather is also essential to the development of design criteria for marine vessels, and coastal and offshore structures. Searches of the literature and discussions with experts in the field (Heidom, 1993) have indicated that little is known about the airflow regime surrounding buoys, their motion in high seas, and the effects of averaging the data on the reporting of a true wind speed.

As a result of the uncertainties concerning wind measurements in sea states where the height of the significant wave is significantly greater than the height of the anemometer, the Storm Wave Study-1 (SWS-1) was initiated. A 6 m ship-shaped NOMAD weather buoy was deployed off the West Coast of British Columbia (approximately 10 miles south-west of Cape St. James) at the southern tip of the Queen Charlotte Islands in 2,000 m of water at WMO location #46147. This buoy, in addition to being part of the regular Canadian network of weather reporting buoys, was equipped with an additional payload designed to gather data (primarily wind speed and direction and wave height and period) at 2 Hz, and store it directly without any averaging.

The buoy was successfully deployed and, in the winter of 1994/95, recorded a number of storms, the worst being associated with a significant wave of 9.4 m. The SWS-1 program is described in Skey *et al.* (1993) and the preliminary analysis of the data was described in Skey *et al.* (1995). Further findings of the SWS-1 data are described here as well as the details of the follow-on SWS-2 study which was initiated as a result of the recommendations from the SWS-1 study.

2.0 SWS PACKAGES

2.1 SWS-1

The SWS-1 package was installed on a standard Environment Canada NOMAD weather buoy. The buoy (WMO location #46147) is part of the network of weather buoys on the West Coast of Canada and, throughout the SWS-1 experimental period, it functioned as a regular buoy transmitting hourly messages as well as supporting the SWS-1 experiment. The SWS-1 package used some of the outputs from the buoy such as wind speed and direction, and wave height.

The SWS-1 program was designed to determine the following:

- whether significant variability in the wind field exists to suggest differences between the vector and scalar wind speeds greater than the 7 to 10% suggested by Gilhousen (1987);
- the extent to which the motion of the buoy increases/reduces the reported wind speed;
- whether high waves shelter the anemometers from the general air flow for a significant portion of the ten-minute averaging period, thus causing a reduced wind speed to be reported;
- the difference between the measured waves calculated from the strap-down accelerometer data and those calculated from the Datawell "gimballed" accelerometer data.

2.2 SWS-2 Package

On Saturday October 25th 1997, a follow up SWS-2 program was initiated with the deployment of an Environment Canada NOMAD buoy at 46°44.05'N, 48°48.13'W on the Grand Banks of Newfoundland in 81m of water on an all-chain mooring, 1.5 nautical miles to the

south-west of the Hibernia platform. The buoy is transmitting regular hourly messages via GOES as well as storing (and transmitting via VHF to the Hibernia platform) the raw SWS-2 data gathered at 2 Hz. The SWS-2 program is based on the recommendations following the analysis of the SWS-1 data.

The main differences between SWS-1 and SWS-2 are:

- an additional strap down accelerometer located as close as possible to the Datawell heave sensor;
- a Solent Windmaster acoustic anemometer, an RMYoung 05305 AQ anemometer as well as an RMYoung 05106 anemometer on the aft mast;
- continuous sampling for period of deployment (c. 6 months) at 2 Hz;
- installation of a 3 Axis Solent Ultrasonic acoustic anemometer on the forward mast. This anemometer is part of a program being run by the Southampton Oceanography Centre;
- SWS-2 located near a fixed platform (Hibernia), a Directional Datawell Waverider and a Minimet Buoy. Data being measured on Hibernia includes wind speed and direction, and wave height and direction from a MIROS wave radar.

The measured parameters for a normally configured NOMAD buoy and for the SWS-1 and SWS-2 payload packages are summarized in Table 2.1.

3.0 WIND

3.1 Vector vs Scalar Winds

The high temporal resolution wind data provided by SWS-1 give an opportunity to investigate vector versus scalar averaging in considerable detail for a continuous range of sample durations in a wide range of sea and wind conditions.

Gilhousen (1986) investigated the difference between vector and scalar averaging of wind speeds by comparing the scalar averaged speeds measured at a C-MAN (Coastal-Marine Automated Network) station on a fixed platform at Chesapeake Light Station, Virginia, with the vector averaged speeds measured by a nearby

Table 2.1
Configuration of NOMAD SWS-1 Buoy (46147) and SWS-2 Buoy (#44153)

Parameter/ System	Normal System for ODAS Buoys	Extra Systems for SWS-1 (WMO Buoy ID #46147) 1994/1995	Extra Systems for SWS-2 (WMO Buoy ID #44153) 1997/1998
Horizontal Wind Speed and Direction	Two RM Young anemometers (model # 05103/6) at 4.45m and 5.25m above sea level (ASL).		Replaced #1 RMYoung anemometer with Solent Windmaster acoustic anemometer. Added an RMYoung AQ on aft extension of aft mast.
Vertical Wind Speed		RM Young anemometer (model #05103), without vane, fixed vertically on horizontal axis 4.82m ASL.	SOC * Solent 3 axis Ultrasonic acoustic anemometer on forward mast.
Vertical Wind Direction		RM Young anemometer (model #05103) on horiz. axis 4.82 m ASL.	SOC * Solent 3 axis Ultrasonic acoustic anemometer on forward mast.
Air temperature	YSI (model #703) with radiation shield at 4.27m ASL.	Increased sampling rate from .5 Hz. to 2 Hz.	Increased sampling rate from .5 Hz. to 2 Hz.
Buoy Attitude		General Oceanics Inc. (model #6011 TAMS) three axis magnetic sensor.	Installed a Systron Donner motion sensor in SWS-2 package.
Wave Height and Period	On west coast - Datawell Mark II heave sensor (single axis vertically stabilised accelerometer); On east coast - strap down accelerometer.	Columbia Research Lab (SA 107B) single axis strap-down accelerometer.	Jewell LCA-100 accelerometer in SWS-2 package and another on top of Datawell sensor.
Barometric Pressure	Atmospheric Instrumentation Research Ltd (model AIR-SB-2A).		
Water Temperature	YSI (model 44203) mounted in a s/s bolt below sea level.		
Compass	Two Systron (model FHS-AV-1) or KVH C100 fluxgate compasses (one for each anemometer).	One Systron (model FHS-AV-1) fluxgate compass.	One KVH C100 fluxgate compass.
Mooring Strain		Metrox TL101-25K tension load link mounted just below bridle.	Metrox TL101-25K tension load link in a modified mounting just below bridle.
Data Acquisition & Processing	ZENO 1200/Watchman 100	SWS-1. Sampling and storage of raw data at 2 Hz under certain weather conditions.	SWS-2. Continuous sampling and storage of raw data at 2 Hz.
Data Transmission	GOES and ARGOS.	Repcos RDS 1200 VHF transceiver.	Repcos RDS 2400 VHF transceiver.

3 m E-Buoy. The fixed platform was equipped with a Bendix Aerovane at a height of at 33.3 m, and the E-Buoy was similarly equipped with a Bendix Aerovane at a height of 3.6 m. For his analysis the wind speeds were adjusted to 10 m. The C-MAN Data Acquisition Control and

Telemetry (DACT) payload for the platform samples wind speed every second for eight minutes. The General Service Buoy Payload (GSBP) used in the E-Buoy takes individual samples of the u and v components every second for 8.5 minutes. Average speed and

direction are then produced from the averaged components. Winds speeds reached 19.5 m/sec and the significant wave height reached 3.5 m for his analysis in extreme conditions with the passage of Hurricane Josephine. While the overall agreement for the buoy and platform speeds is good (the SD of the difference between the buoy and platform speeds is about the same as the SD of the difference between the platform's two anemometers), the buoy speeds are lower than the platform speeds for high wind speed events due to the averaging methods. Subsequent comparison of both averaging methods for the same anemometer at buoy station 41001 indicated that for speeds greater than 8 m/sec, the vector averaged speeds were about 7% lower than the scalar averaged speeds.

3.1.1 Calculation of SWS-1 Mean Wind Speeds

The SWS-1 anemometers are referenced directly to the fluxgate compass which is used for determining buoy heading. Both anemometers are referenced to the same compass, eliminating the source of error introduced if separate compasses were used. As the yaw component of buoy motion induces an apparent directional change in an otherwise stationary anemometer due to this directional reference, the buoy heading is subtracted from the wind direction value to provide true wind direction corrected for platform yaw.

From the SWS-1 data set instantaneous scalar wind speed s_i and direction θ_i are computed from the 2.0 Hz output of the independent pulse counters into which are fed the frequency outputs of the port and starboard anemometers by dividing the integer values p_s and p_θ in the digital pulse counter by the sample interval L (Eqns. 1, 2). The difference in sample frequency from the standard ZENO processing has no effect on the calculation of scalar wind speed values for sample duration of equal length which are greater than the ZENO sampling period.

$$s_i = \left(\sum_{t=0}^{t=L} p_s \right) / L \quad (1)$$

$$\theta_i = \left(\sum_{t=0}^{t=L} p_\theta \right) / L \quad (2)$$

The scalar wind speed u is computed by dividing the sum of the resultant instantaneous wind speeds s_i by the number of samples n in the sample duration (Eqn. 3)

$$u = \left(\sum_{i=1}^n s_i \right) / n \quad (3)$$

Vector wind speeds \bar{v} are determined from the SWS-1 data set by computing the v_x and v_y components of the corrected wind direction and averaged over the number of samples n in the appropriate gust length for instantaneous speed s_i and instantaneous wind direction θ_i (Eqns. 4a-4f).

$$v_{xi} = v(\sin \theta_i) \quad (4a)$$

$$v_{yi} = v(\cos \theta_i) \quad (4b)$$

$$\bar{v}_x = \left(\sum_{i=1}^n v_{xi} \right) / n \quad (4c)$$

$$\bar{v}_y = \left(\sum_{i=1}^n v_{yi} \right) / n \quad (4d)$$

$$\bar{v} = \sqrt{\bar{v}_x^2 + \bar{v}_y^2} \quad (4e)$$

$$\bar{\theta} = 270 - \arctan(\bar{v}_y / \bar{v}_x) \quad (4f)$$

3.1.2 Comparison of 10-Minute Vector and Scalar Means

Running 10-minute vector and scalar means (v_{10} , u_{10}) are computed at one minute intervals for entire storms and the percentage difference

δ calculated (Eqn. 5). A typical time series is provided in Figure 3-1. Percentage differences between the vector and scalar values for all storms are summarized in Table 3.1.

$$\delta = 100 \left(\frac{(u_{10} - v_{10})}{u_{10}} \right) \quad (5)$$

The average difference for all storms as reported in Table 3.1 is 3.1%, and is as low as 0.9% for the low wind and wave conditions of March 06, 1994. The only event that approximates Gillhousen's 7% value is the 8.61% value for the storm of December 05, 1994, which deserves closer investigation.

Time series plots of δ for this storm indicate two areas in which the difference exceeds an otherwise lower than average value of 2%. The first event is a sharp spike of an approximate magnitude of 35% which occurs just before the 4th hour of the storm; the second event is an increasing difference (which peaks at 70%) from hour 6 to the end of the data record. When this difference is plotted against the 10-minute scalar wind speed it becomes apparent that the spiking beyond hour 6 is attributable to the nature of the difference calculation in that the absolute value of the wind speed drops nearly to zero, causing any wind speed difference of a constant absolute magnitude to increase as a proportion of the diminishing absolute wind speed. This accounts for the spiking beyond hour 6 which can be ignored as the difference calculation becomes an inappropriate statistic for near-zero wind conditions.

When plotted against the 10-minute mean wind direction for the storm of December 05, 1994, the difference spike just prior to the 4th hour of the storm coincides with an abrupt change in wind direction of approximately 140° in 10 minutes. Inspection of the 10-minute scalar mean wind speed reveals a significant change in scalar wind speed at the same point. Surface Analysis Charts provided by Environment Canada's Pacific Weather Centre for 0600Z and 1200Z December 05, 1994 indicate that a frontal system passed over the SWS-1 moored buoy sometime between the two reports. This demonstrates that the first spike is attributable to the recording of a legitimate meteorological event.

Overall, the difference between 10-minute vector and scalar wind speeds are lower than anticipated in the extreme sea states recorded by SWS-1. While vector averaging is intuitively dependent on the high frequency variability of wind direction, further analysis of the wave sheltering effect on both wind speed and direction over individual waves suggests that the unexpectedly low difference between vector and scalar winds is partially attributable to the joint distribution of the high frequency variability of both wind speed and wind direction.

3.1.3 Comparison of Scalar and Vector Gusts

As high frequency variability in wind direction contributes to lower reported values of vector versus scalar 10-minute mean winds, it likewise contributes to lower values of vector versus scalar gusts of shorter periods. The algorithm for the computation of gusts is similar to that of the 10-minute mean (Eqns. 3, 4). The percentage difference δ (Eqn. 5) as a function of relative and cumulative frequency was computed for gusts of both five and eight seconds duration ($L = 5$, $L = 8$). Scalar and vector gusts were computed at one-second intervals for the duration of the storm of November 04, 1994, with over 86,000 points in the population sample. The difference distribution δ of this storm is representative of all the storms collected in the SWS-1 data set. Over 40% of both eight and five second gusts are within 0.5% of each other, independent of wind speed, wave height, or variability of wind direction. The cumulative frequency portion of the graph indicates that 95% of vector and scalar gust values are within 4% and 5% of each other for gusts of five and eight seconds respectively. This suggests that there is not a significant difference between the calculation of gusts (vector or scalar) for duration of five seconds (some of the US platforms) and eight seconds (the Canadian buoy network - now changing over to 5 second gusts).

3.2 Gust Factor Analysis

The gust g_L of a sample is defined as the maximum scalar wind speed u_L of duration L over a record of period T (Eqn. 6).

$$g_L = \max(u_L) \Big|_{t=0}^{t=T} \quad (6)$$

The gust factors f_{uL} and f_{vL} are defined as the ratio of the gust g_L to the scalar mean \bar{u}_T and vector mean \bar{v}_T of period T (Eqns. 7, 8).

$$f_{uL} = \frac{g_L}{u_T} \quad (7)$$

$$f_{vL} = \frac{g_L}{v_T} \quad (8)$$

A relation of gust factors as a function of sample duration was plotted by averaging all of the scalar gust factor values f_{uL} and f_{vL} over a given sample duration from $L=0.5$ to $L=30.0$ seconds for a period $T=10$ minutes, with $n=727$ samples in the population (Eqns. 9, 10).

$$R_{uL} = \frac{\sum_{i=1}^n f_{uL}}{n} \quad (9)$$

$$R_{vL} = \frac{\sum_{i=1}^n f_{vL}}{n} \quad (10)$$

When plotted against sample duration L , mean gust factors R_{uL} and R_{vL} describe a general relation which might be used as a data quality control index for determining the validity of reported scalar gust values given the 10-minute vector or scalar mean wind speed (Figure 3-2). For sample duration $L=8$ seconds, a scatter plot of f_{uL} and f_{vL} versus scalar and vector wind speeds (Figures 11,12) indicates the factor distribution and suggests a constant relation for wind speeds in excess of approximately 7 to 8 m/sec, with $f_{uL}=1.23$ (SD=0.08) and $f_{vL}=1.27$ (SD=0.11). The data for these calculations came from the November 4th storm.

Table 3.1
Scalar vs. Vector Wind Speeds
Mean of 10-Minute Averages Computed Every One Minute

Date	Starboard						Port					
	Scalar u (m/s)	Scalar std dev	Vector u (m/s)	Vector std dev	% Diff.	% Diff. std dev	Scalar u (m/s)	Scalar std dev	Vector u (m/s)	Vector std dev	% Diff.	% Diff. std dev
Nov04/94	11.92	2.35	11.54	2.3	3.45	1	11	3.04	10.65	2.97	3.43	1.09
Nov06/94	8.16	1.19	7.83	1.11	4.29	1.3	7.44	1.72	7.14	1.67	4.26	1.24
Nov12/94	8.68	1.42	8.43	1.43	3.08	1.53	7.79	2.47	7.58	2.43	2.82	0.81
Nov14/94	9.39	0.82	9.2	0.83	2.11	0.51	8.84	0.6	8.66	0.61	2.2	0.58
Nov27/94	11.36	1.2	10.89	1.24	4.39	3.05	10.96	1.17	10.67	1.13	2.74	0.56
Nov30/94	12.94	1.9	12.63	1.86	2.45	0.41	12.47	1.79	12.17	1.75	2.52	0.43
Dec02/94	9.69	2.79	9.35	2.71	3.78	1.34	9.4	2.8	9.08	2.7	3.56	0.81
Dec05/94	10.77	6.95	10.22	6.7	8.61	8.19	10.62	7	6.17	6.82	7.23	6.64
Dec06/94	7.44	2.61	7.2	2.64	4.24	3.03	6.99	2.65	6.76	2.67	4.32	3.04
Dec07/94	8.68	1.08	8.43	1.06	2.95	0.6	8.45	1.07	8.2	1.04	3.06	0.6
Dec19/94	10.98	1.46	10.69	1.44	2.77	0.63	11.05	1.42	10.76	1.39	2.74	0.6
Dec22/94	15.97	1.24	15.57	1.21	2.56	0.45	16.07	1.28	15.67	1.25	2.53	0.43
Dec30/94	6.96	0.74	6.76	0.47	3.08	0.43	6.76	0.45	6.62	0.45	2.09	0.32
Jan 15/95	11.9	0.9	11.6	0.9	2.63	0.66	11.92	0.91	11.59	0.92	2.82	0.79
Jan 18/95	4.7	0.44	5.69	0.44	1.64	0.41	6.61	0.43	6.5	0.43	1.75	0.37
Jan 24/95	14.79	3.92	14.24	3.72	3.77	0.84	14.53	3.9	13.99	3.69	3.75	0.94
Feb 10/95	10.61	0.64	10.48	0.64	1.2	0.21	9.77	0.68	9.66	0.68	1.1	0.21
Mar06/95	7.31	0.57	7.25	0.57	0.9	0.1	7.2	0.57	7.13	0.56	1.07	0.13
Mar29/95	10.43	0.38	10.28	0.38	1.55	0.13	9.98	0.39	9.93	0.38	1.53	0.11

3.3 Variability of Wind Speed and Direction

The flow of air over waves in extreme sea states is a complex issue. There is little data currently available to describe in detail the flow regime over individual waves as measured by a moored buoy.

Jeffreys (Sverdrup *et al.*, 1942; Wiegel, 1964) theorized that the flow field will exhibit separation behind solid obstacles (i.e., waves) due to eddy formation resulting from unequal air pressures on the windward and leeward sides of a perturbation of the water surface. This effect can only prevail when waves travel at a velocity smaller than the wind speed (Sverdrup *et al.*, 1942). Another school of thought contends that wind speed is unaffected by the waves in fully developed seas (wave speed equals wind speed) and that if waves affect the wind measurements, they do so by physical action on the buoy including knocking the buoy over by breaking waves (Heidorn, 1993).

The predictions of various theories of wind behaviour in high sea states are largely qualitative, and while this study may not definitively determine which models are correct, it provides data which can be used to quantify the magnitude of the various effects postulated.

Examination of wind direction over individual waves indicates significant variability. This variability typically decreases as a function of wave height. Zero crossing analysis is used to compute the joint distribution of the change in wind direction over an individual wave, with the frequency of these events for all storms summarized in Table 3.2. When the mean change in wind direction is computed as a function of wave height, a well-defined linear relationship becomes evident, with average changes of over 80° for wave heights in excess of 14 m (Figure 3-3). Regression coefficients for the fit of this relation are $m=3.6$ and $b=30.0$.

Wind speed demonstrates a similar degree of variability over individual waves in high sea states. While the wind speed appears to track the wave field quite closely in higher sea states, this correlation decreases in calmer seas. Table 3.3 contains the joint distribution of the decrease in wind speed and wave height for all storms. The decrease in speed is expressed as the percentage drop from the maximum

instantaneous wind speed on the crest to the lowest instantaneous wind speed in the trough over a period of each corresponding zero crossing event. The mean decrease in wind speed calculated in this manner as a function of wave height is provided in Figure 3-4. Again a linear relation becomes evident, with regression coefficients of $m=2.29$ and $b=16.2$.

3.4 Effects of Buoy Motion on Wind Measurements

Another of the objectives of the SWS-1 project was to determine the effects of buoy motion in extreme sea states on reported wind speeds. Pond (1968) found that for buoy tilts of less than 10°, errors in wind speeds due to the varying tilt of the mast are negligible (less than 3%), increasing to 15% and 23% for tilts of 23° and 29° respectively. For the NOMAD hull design, Gilhousen (1986) computed the pitch response amplitude operators (RAOs), expressed in terms of degrees of pitch per meter of wave height, as a function of wave frequency. He found that the average pitch angles do not increase much for significant wave heights between three and 13 m, with the angles below 10° for significant wave heights under 11 m.

On the Canadian NOMAD buoys (including the SWS-1 buoy), the anemometers are fixed to the rear mast approximately 3.28 m aft of the centre of rotation (the bridle) at 4.45 m and 5.25 m elevation above the water line. With the centre of rotation 1.87 m below the water line, the effective length of the moment arm of the anemometers is 7.12 m and 7.48 m. The average additional induced wind speed (caused by the buoy motion on the anemometer) is computed for total tilts of 10°, 20°, 30° and 40° over a range of wave periods (Figure 3-5). As the degree of platform roll is symmetrical, it can be assumed that the pumping effect is approximately symmetrical over the individual wave with a zero net effect (vector averaged) as the anemometer accelerates into and out of the wind field. Maximum scalar values for this effect of less than 1.0 m/sec suggest that the larger variations in wind velocities over individual waves are attributable to sources other than buoy motion.

Examination of the magnetometer data from the November 4th storm indicates maximum

Table 3.2
Change in Wind Direction vs. Wave Height

180	0	0	0	0	0	0	0	0	0	0	0	0	0	0	0	0
170	3	21	31	39	45	27	25	15	10	3	1	2	1	1	0	0
160	5	18	38	32	31	34	25	16	10	7	0	2	0	1	1	0
150	6	14	27	44	48	37	27	17	11	2	4	0	1	0	0	0
140	9	19	30	36	35	38	25	19	5	7	2	2	0	0	0	0
130	7	24	46	53	54	46	41	22	19	12	2	4	1	0	0	0
120	8	21	44	57	81	50	35	30	20	12	3	2	1	2	0	0
110	12	39	63	57	73	47	51	32	22	16	4	4	3	2	2	1
100	12	30	67	74	97	91	65	44	45	21	11	7	7	0	1	0
90	9	53	87	113	127	136	104	81	67	49	35	16	11	6	2	0
80	14	76	130	181	204	230	177	161	115	93	52	32	15	13	1	0
70	33	127	244	328	409	425	422	345	235	161	99	51	25	11	3	1
60	55	215	469	720	958	1056	906	729	480	249	169	60	29	19	2	1
50	102	488	1170	1706	2081	2040	1616	1026	632	340	144	53	15	7	4	0
40	318	1330	2562	3558	3586	3080	2082	1122	550	239	106	38	14	5	1	0
30	871	3184	4458	4561	3842	2610	1476	687	300	105	49	22	6	2	1	0
20	1859	4275	4041	2689	1721	900	471	189	76	26	14	4	1	0	0	0
10	2067	2133	1061	442	213	87	35	14	6	3	2	1	0	0	0	0
0	625	133	52	39	28	13	12	3	4	1	2	0	0	0	0	0
	0	1	2	3	4	5	6	7	8	9	10	11	12	13	14	15

Wave Height (m)

Table 3.3
Percentage Decrease in Wind Speed from Maximum Crest Speed vs. Wave Height (m)

100	32	85	167	198	227	150	105	57	22	18	6	3	4	1	0	0	0
90	3	9	6	14	13	15	6	3	6	3	0	2	1	0	0	0	1
80	0	3	10	10	17	13	4	4	0	2	2	1	1	1	0	0	0
70	4	5	7	15	13	13	5	9	10	13	10	7	7	5	1	0	1
60	4	12	13	16	34	58	73	69	72	56	42	26	14	7	4	0	0
50	4	21	61	138	265	386	442	364	260	189	91	46	14	11	5	0	1
40	12	134	447	889	1338	1539	1269	946	600	309	193	85	37	16	4	1	1
30	173	958	2111	3272	3844	3294	2317	1465	857	436	187	80	24	10	3	0	0
20	906	3241	4994	5247	4708	3499	2267	1167	560	254	126	39	16	13	2	2	0
10	2083	4408	4502	3569	2526	1584	850	406	191	73	38	8	11	4	0	0	0
0	2682	3129	2210	1348	749	391	210	84	32	9	4	3	1	0	0	0	0
	0	1	2	3	4	5	6	7	8	9	10	11	12	13	14	15	16

Wave Height (m)

total tilt values on the order of 60° for pitch and 35° for roll for individual extreme waves. Ninety-nine percent of roll and pitch values were recorded as being less than 30°.

4.0 Comparison of Heave Sensors

Both the Datawell gimbaled heave sensor and the Columbia strap-down accelerometer are used to measure wave height in the Canadian data buoy network. While the NOMAD platforms on the West Coast are equipped with Datawell heave sensors, accelerometers are used in nearly all of the East Coast buoys. Concurrent sampling of the gimbaled Datawell

heave sensor and the strap-down Columbia accelerometer in SWS-1 permit direct intercomparison of the output of these sensors in extreme sea states. The off-angle response of the accelerometer is believed to contribute to an under-reporting by the accelerometer of wave height because the gravitational component of the output is reduced as the platform is tilted from a level of orientation. Sensor acceleration is doubly integrated to produce displacement values for both sensors.

Time series of the output of the two heave sensors demonstrate that overall the accelerometer reports lower values of heave than the Datawell, independent of sea state.

When the full frequency output of Datawell versus accelerometer heave values for the storm of 4 November 1994, (a data set comprised of over 86,000 data points) is plotted, there is a heave correlation of 0.85, and the slope of the accelerometer values relative to the Datawell values is 0.88. This relation is characteristic of all the storms collected by the SWS-1 package. When the mean value of the difference between the Datawell and the accelerometer is plotted as a function of wave height, it becomes evident that there is a linear relationship (Figure 4-1). For wave heights greater than 13 m, the linear relationship seems to break down, however the number of events in this range is very low (Table 4.1). This relationship, when expressed as a percentage mean difference between the two sensors and plotted against the individual trough to crest wave heights, is shown in Figure 26 for all SWS-1 storms. The difference increases steadily from about 2% or 3% for waves in the 2 m range, to about 10% for waves greater than 10 m. Beyond 13 m or so there are relatively little data and a corresponding decrease in the confidence of the results.

4.1 Calculation of Maximum Wave

The maximum positive wave amplitude (wave crest to mean sea level) is of considerable interest to the marine engineer computing the environmental loading factors in

the design of offshore structures as project costs rapidly increase with wave height and air gap requirements. The wave analysis in the Canadian data buoy network assumes that the wave shape is symmetrical and reports a value for the maximum wave height, Hmax, which is calculated as twice the maximum positive wave amplitude. When the ratio of the total wave height (crest to trough) to the positive wave amplitude is plotted as a function of the total wave height for the Datawell sensor, it falls below 2.0 for wave heights exceeding 8 m, confirming that in extreme sea states the wave shape is not symmetrical. Thus, the Hmax as reported by some of the buoys in the Canadian network is misleading as an index of total wave height in extreme seas.

Over the next few years the processing packages in the Canadian buoys will change from a ZENO to a Watchman 100. The wave analysis software in the Watchman returns a true peak to trough value for the maximum wave. The key to determining whether a particular buoy is fitted with Watchman or a ZENO payload lies in the 912 maximum wind speed indicator group in the WMO formatted message. The key is as follows:

- If the maximum speed indicator group reads **921** then the payload is a ZENO and the maximum wave is calculated as twice the crest height.

**Table 4.1
Datawell/Accelerometer Comparison (All Storms)**

Wave Height (m)	Difference (m)	Difference (%)	Number of Events
0	-0.25	-81.05	2,354
1	-0.06	-6.0	11,324
2	0.06	2.98	16,059
3	0.16	5.24	17,886
4	0.26	6.57	17,348
5	0.37	7.44	15,220
6	0.47	7.84	11,131
7	0.58	8.38	7,076
8	0.71	8.89	4,225
9	0.8	8.95	2,280
10	0.96	9.68	1,182
11	1.05	9.6	550
12	1.42	11.94	232
13	1.29	10.0	119
14	2.03	14.64	48
15	2.49	16.67	9
16	-0.06	-0.36	6

- If the maximum speed indicator group reads **912** then the payload is a Watchman 100 and the maximum wave is reported as the greatest measured value of the peak to trough.

5.0 CONCLUSIONS AND RECOMMENDATIONS

5.1 Conclusions

In summary the data from SWS-1 data showed a number of interesting and important results. These were:

- wind speed and direction both demonstrated significant variabilities over individual waves. The so-called sheltering effect manifesting itself with reduced speeds and changes in wind direction in the wave troughs. These variabilities typically increased with increasing wave height. These variabilities were shown to have linear relationships with wave height;
- the effect of reporting vector mean winds as opposed to scalar mean winds seems to make a difference of only 3% or 4%. This is less than the 7% proposed by Gilhousen;
- the effect of the roll and pitch motions of the buoy had a negligible effect on the reported wind speeds;
- the strap-down accelerometer appears to read about 10% lower than the Datawell Mark II sensor under most wave conditions; and,
- the variability of wind and wave conditions within any one hour is quite large. The data that are reported on the hourly satellite broadcast is thus a factor of the conditions encountered, the sampling and averaging interval, and the processing algorithms.

Preliminary SWS-2 data from a three week period from the end of November/early December 1997 will be presented at the workshop if possible.

6.0 REFERENCES

Axys Environmental Consulting Ltd. 1996. Meteorological and Oceanographic Measurements from Canadian Weather Buoys. A review of sensors, data reduction, transmission, quality control and archival

method. Environment Canada, Downsview, Ontario, March 1996. 43 pp.

Bigio, R. 1992. A sampling of damage reports from the Halloween 1991 Storm, Supplement - Proceedings of the 3rd International Workshop on Wave Hindcasting and Forecasting, Montreal, Quebec, May 1992. Atmospheric Environment Service, Environment Canada, Downsview, Ontario, pp. 45-70.

Cardone, V.J. and B.T. Callahan. 1992. Kinematic analysis of the surface wind field in the Halloween Storm and a preliminary spectral model wave hindcast, Supplement - Proceedings of the 3rd International Workshop on Wave Hindcasting and Forecasting, Montreal, Quebec, May 1992. Atmospheric Environment Service, Environment Canada, Downsview, Ontario, pp. 101-118.

Cardone, V.J., and V.R. Swail. 1995. Uncertainty in Prediction of Extreme Storm Seas (ESS). Proceedings of the 4th International Workshop on Wave Hindcasting and Forecasting, Bann, Alberta, October 16-20, 1995. Environment Canada, pp. 1-20.

Earle, M.D. and J.M. Bishop. 1984. A Practical Guide to Ocean Wave Measurement and Analysis. Endeco, Inc., Marion, MA. 80pp.

Gilhousen, D.B. 1986. An accuracy statement for meteorological measurements obtained from NDBC moored buoys. National Data Buoy Center, NSTL, MS 39529.

Gilhousen, D.B. 1987. A Field Evaluation of NDBC Moored Buoy Winds. J. Atmos. Ocean. Technol., 4:94-104.

Heidorn, K.C. 1993. The Influence of High Waves on Buoy-Measured Wind Speeds. Atmospheric Environment Service, Environment Canada, Downsview, Ontario.

Pond, S. 1968. Some Effects of Buoy Motion on Measurements of Wind Speed and Stress. Journal of Geophysical Research, Vol. 73, No. 2:507-512.

Skey, S.G.P., K.C. Heidorn, S. Jarvin and V.R. Swail. 1993. The Measurement of Wind Speed in High Seas by Meteorological Buoys. Oceans '93, Victoria, B.C. IEEE.

Skey, S.G.P., K. Berger-North, V.R. Swail. 1995. Detailed measurement of winds and waves in high seastates from a moored NOMAD weather buoy. Proceedings of the 4th International Workshop on Wave Hindcasting and

Forecasting, Banff, Alberta, October 16-20,
1995. Environment Canada, pp. 213-223.

Sverdrup, H.U., M.W. Johnson, and R.H. Fleming.
1942. The Oceans: Their Physics, Chemistry
and General Biology. Prentice-Hall Inc.,
Englewood Cliffs, NJ. 1087pp.

Wiegel, R.L. 1964. Ocean Engineering. Prentice-
Hall, Inc., Englewood, NJ. 532pp.

Personal Communications

Dr. Vincent J. Cardone, President
Oceanweather Inc., Suite 1, 5 River Road, Cos
Cob, CT 06807, USA.

Mr. Ken Steele
National Data Buoy Centre, NOAA, Stennis
Space Centre, Bay St. Louis, Mississippi.

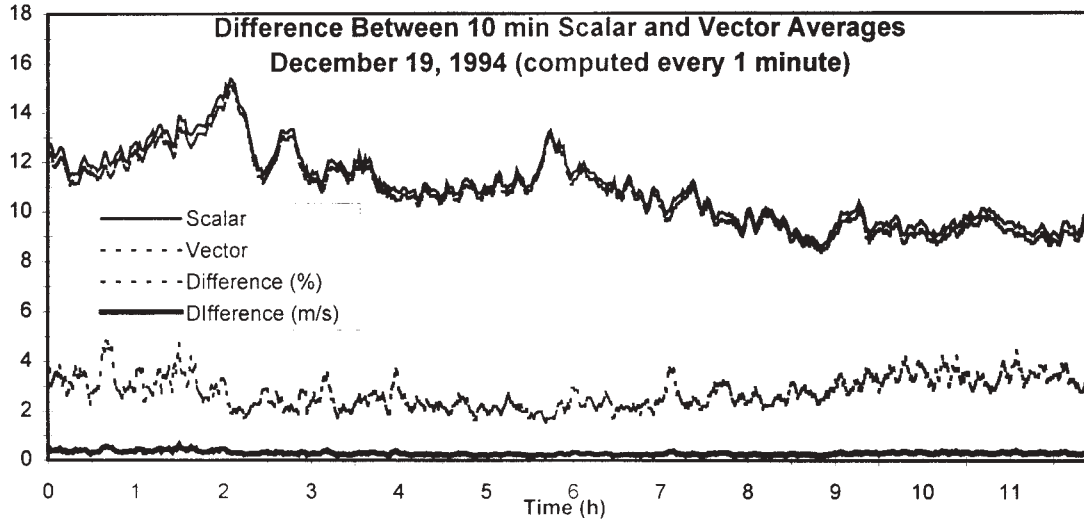


Figure 3-1

Scalar Gust Factors vs Gust Length

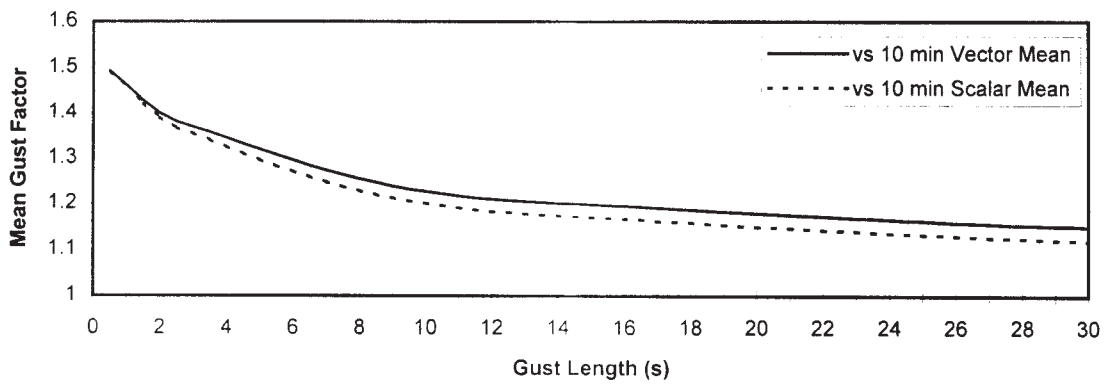


Figure 3-2

Mean Change in Buoy Heading

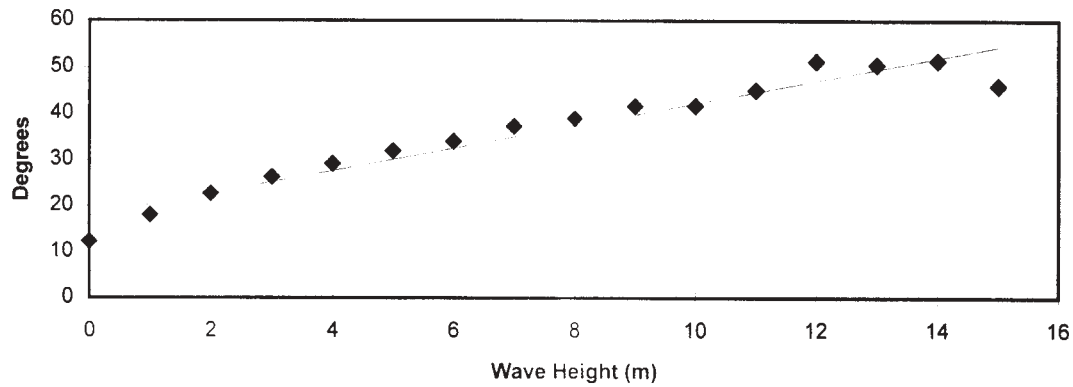


Figure 3-3

Mean Decrease in Wind Speed (All Storms)

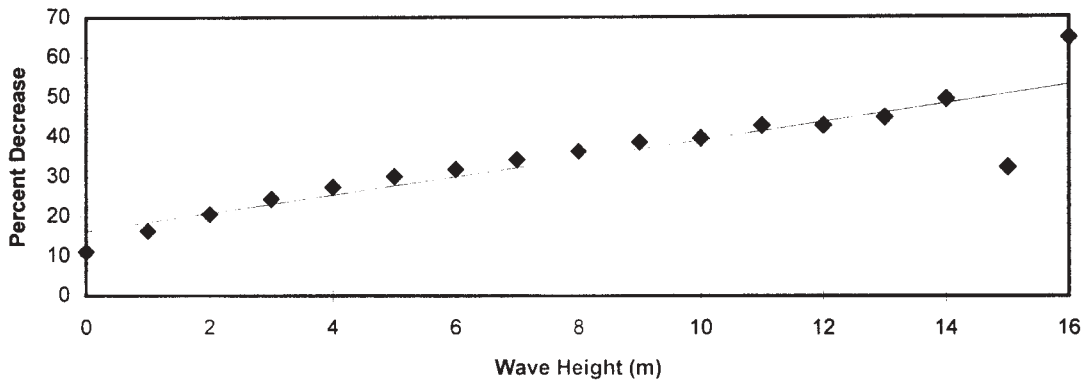


Figure 3-4

Anemometer Pumping vs Wave Period

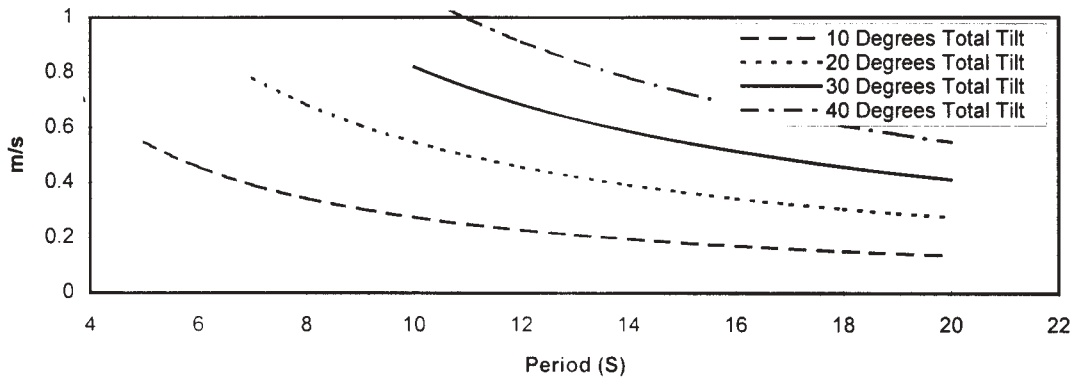


Figure 3-5

Datawell / Accelerometer Agreement (All Storms)

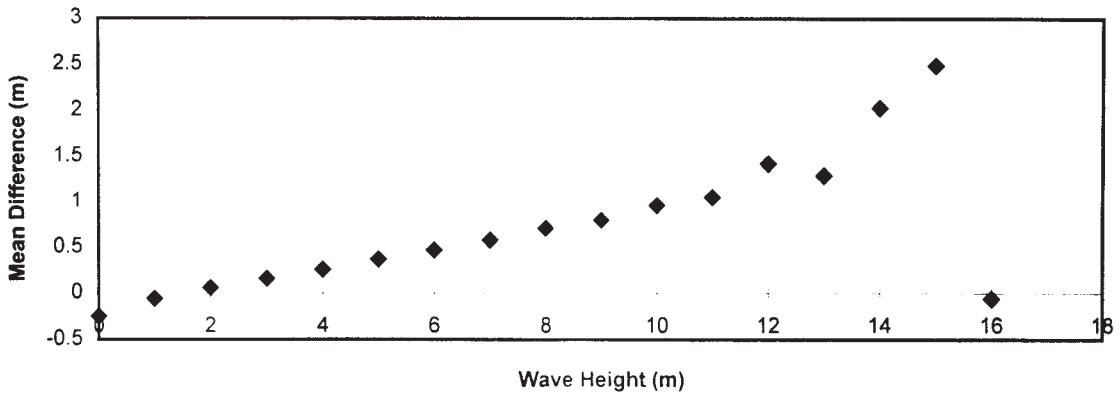


Figure 4-1